Journal of Engineering Science and Technology Review 16 (6) (2023) 108 - 116

Research Article

JOURNAL OF
Engineering Science and Technology Review

www.jestr.org

Elastoplastic Solution of TBM Inclined Shaft Surrounding Rocks under Non-constant Pressure with Consideration of Intermediate Principal Stress

Lulu Liu[1], Junyuan Yan[1,*] and Shenggaoya Cao[2]

[1]*College of Civil Engineering and Architecture, Qingdao Agricultural University, Qingdao 266109, China*
[2] *School of Environment, Education and Development, The University of Manchester, Manchester, M13 9PL, United Kingdom*

Received 13 August 2023; Accepted 19 November 2023

Abstract

Long-distance Tunnel Boring Machine (TBM) inclined shaft is characteristic of great changes in buried depth, large slope, and running across complicated formation. Stresses in the support and surrounding rocks after the inclined shaft excavation are obviously different from those in horizontal tunnels. Thus far, studies on stresses of inclined shafts are limited. To investigate the mechanical properties of lining-surrounding rocks in TBM inclined shaft systematically, a mechanical analysis model of TBM inclined shaft under non-constant pressure was established. The elastoplastic solution of surrounding rocks in inclined shaft was solved based on unified strength theory. Expressions of surrounding rock stresses, displacements, and the plastic zone radius with comprehensive considerations to intermediate principal stress (described by the influencing factor (b) of intermediate principal stress), lateral pressure coefficient (K_0) of surrounding rocks, angle of the inclined shaft, and elasticity modulus of lining were deduced. Moreover, a computational analysis based on an engineering case was performed. Results demonstrate that, surrounding rocks are more stable if the intermediate principal stress makes greater contributions. The value of b increases from 0 to 1, whereas the plastic zone radius of surrounding rocks and the radial displacement of tunnel wall decrease by 9.96% and 18%, respectively. The K_0 considerably affects the radius and displacement of the plastic zone on surrounding rocks along different directions. When b=1 and K_0 increases from 0.8 to 1.2, the horizontal displacement of the tunnel wall increases by 40%. A larger angle of the inclined shaft has more significant influences on the radius and displacement of the plastic zone. With the increase in the elasticity modulus of lining, the radius and radial displacement of the plastic zone decrease accordingly. The proposed model provides important theoretical references to safety analysis and support scheme selection for surrounding rocks in similar TBM inclined shaft projects.

Keywords: Elastoplastic solution, Unified strength theory, Angle of inclined shaft, Lateral pressure coefficient, Elasticity modulus of lining

1. Introduction

With the development of scientific technology and mechanized construction, Tunnel Boring Machine (TBM) becomes the first choice of long-distance inclined shaft engineering due to its advantages of safety, high-efficiency, and fast construction [1]. In the construction process of long-distance TBM inclined shaft, it may encounter many problems, such as large angle, varying buried depth, and running across complicated formation. With the increase of buried depth, influences of above factors on the stability of surrounding rocks will intensify gradually. Surrounding rocks are in initial stress state before excavation of the inclined shaft. However, stresses in surrounding rocks will be redistributed after excavation, and local rocks enter into the plastic state, which require immediate support. Moreover, certain requirements must be met concerning the strength of the support structure. How to analyze and evaluate the stability of surrounding rocks and safety of support structure after excavation is of important significance to engineering.

The mechanics of lining and surrounding rocks in long-distance TBM inclined shaft systematically must be investigated for an accurate understanding of the deformation of surrounding rocks and for the selection of an appropriate lining structure. Many scholars have performed elastoplastic theoretical studies of surrounding rocks in deeply buried horizontal tunnels under constant pressure by using Mohr–Coulomb (M–C) strength criterion [2-3] and Hoek–Brown (H–B) strength criterion [4-5]. However, they have ignored the differences between horizontal and vertical pressures of surrounding rocks. When TBM inclined shaft advances to a deep position, stresses on surrounding rocks are different from those at shallow positions and they might be influenced by tectonic stresses. The horizontal stress is generally unequal to vertical stress. Some scholars have investigated mechanics of circular roadway surrounding rock under non-constant pressure by using the different failure criteria, and analyzed influencing laws of lateral pressure coefficient of surrounding rocks reasonably [6-7]. However, they have ignored the influences of the intermediate principal stress. Tests have shown that the influence of intermediate principal stress on the yield strength of rocks cannot be ignored. Research results of mechanical properties of surrounding rocks with considerations to the influence of intermediate principal stress conform better to practical situations [8]. Some scholars have conducted theoretical analyses on surrounding rocks in horizontal circular tunnel with considerations to intermediate principal stress. They have discussed the influencing laws of intermediate principal stress on the plastic range of surrounding rocks. However, they have not

*E-mail address: yanjunyuan88@163.com

doi:10.25103/jestr.166.13

thoroughly analyzed the displacement of surrounding rocks [9]. Stresses in surrounding rocks and support structure in TBM inclined shaft are more complicated and have important influences on engineering safety. Existing theoretical research results cannot be applied to TBM inclined shaft engineering completely. Therefore, the mechanical properties of lining-surrounding rocks in TBM inclined shaft must be further investigated and analyzed.

With considerations to the characteristics of TBM inclined shaft engineering, a mechanical analysis model of lining-surrounding rocks in deeply buried TBM inclined shaft is constructed, which is used for a systematic mechanical analysis of elastoplasticity. Variation laws of the mechanical properties of surrounding rocks with angle of the inclined shaft, intermediate principal stress, lateral pressure coefficient of surrounding rocks, and elasticity modulus of lining are also discussed.

2. State of the Art

Existing studies on the stability of surrounding rocks in deeply buried tunnels have mainly focused on the variation laws of stresses, range of the plastic zone, and displacement of surrounding rocks, and most of them have selected horizontal tunnels as their research object. Park [10] theoretically solved the surrounding rocks of horizontal tunnels based on M–C and H–B strength criteria. They also analyzed the influencing laws of the initial stress of surrounding rocks on the radius and radial displacement of the plastic zone. Singh et al. [11] proposed the analytical solution to the surrounding rocks of deeply buried tunnels based on the Mogi–Coulomb failure criterion and analyzed parameters. The results showed that the influence of Poisson's ratio on the stress and displacement of surrounding rocks is insignificant, and the dilatancy angle can directly affect the displacement of surrounding rocks. Hedayat et al. [12] proposed a new analytical–numerical calculation method to analyze the elastoplastic zone of surrounding rocks in tunnels. They found that the dead load of rock mass and crushing zone have important influences on the convergence and stress distribution of surrounding rocks. Adhikari et al. [13] performed a mechanical analysis on the surrounding rocks of circular tunnels in rocks based on a finite element model and H–B failure criterion. They found that the lateral pressure coefficient of surrounding rocks can influence the distribution of plastic zone. Ma et al. [14] solved the stress of surrounding rocks and the range of plastic zone in deeply buried circular tunnels using a conformal mapping method and complex theory. They analyzed the influencing laws of the lateral pressure coefficient on the range of plastic zone. Chen et al. [15] deduced the calculation formulas of the stresses and displacements of surrounding rocks in deep circular tunnels using large deformation theory and three-dimensional H–B yield criterion. The results showed that the intermediate principal stress and support force significantly affect the range and radial displacement of the plastic zone. Ma et al. [16] deduced the calculation of deviator stresses and plastic zone radius around circular roadway under non-constant pressure. They discussed the influences of lateral pressure coefficient, internal friction angle and tunnel radius on plastic zone radius. Behnam et al. [17] studied the range of the plastic zone of surrounding rocks in circular tunnels based on the H–B failure criterion and gained the calculation formula of the plastic zone radius. With considerations to the strain softening characteristics of rocks, Lee et al. [18] investigated the variation laws of the stresses and displacements of surrounding rocks in circular tunnels based on M–C and the generalized H–B strength criterion. They also performed an experimental verification through numerical calculation. Zeng et al. [19] conducted a mechanical analysis of surrounding rocks in circular tunnels under non-constant pressure condition and deduced the elastoplastic solution to surrounding rocks based on unified strength theory and non-associated flow rule. They discussed the influencing laws of lateral pressure coefficient and intermediate principal stress on the plastic zone radius and the displacement of tunnel wall. These elastoplastic theoretical studies on the surrounding rocks and support structure of horizontal tunnels focused on the influences of the lateral pressure coefficient of surrounding rocks and intermediate principal stress on the range and displacement of plastic zone. Nevertheless, none of them thoroughly analyzed the effect of lining on surrounding rocks. The influencing laws of the lining elasticity modulus on the range and displacement of the plastic zone of surrounding rocks still remain unknown.

Scholars have paid more attention to construction technologies in TBM inclined shaft engineering. Yuan et al. [20] proposed the comprehensive technologies to improve the strength of surrounding rocks in inclined shaft. Qiao et al. [21] performed structural and functional analyses of the material lifting system in inclined shaft. They designed reasonable control, monitoring, and protection systems. Fan et al. [22] built a full mine mechanical advancing and shaft building system for Kekegai Coal Mine, which increased the advancing efficiency significantly. These studies involved multiple technological improvement and increased construction safety and efficiency of TBM inclined shaft engineering significantly. However, they lacked a systematic mechanical analysis of lining-surrounding rocks in TBM inclined shaft. Moreover, the influencing laws of inclined shaft inclination angle on the mechanical properties of surrounding rocks still remain unclear.

To address the above problems, an elastoplastic mechanical analysis model in the cross section of a deeply buried TBM inclined shaft is constructed by combining the coordinate transformation theory, with comprehensive considerations to inclined shaft inclination angle, intermediate principal stress, lateral pressure of surrounding rocks, and elasticity modulus of lining. An elastoplastic solution is derived based on unified strength theory. A parameter analysis is conducted by combining the data of a TBM inclined shaft project. The influencing laws of intermediate principal stress, inclined shaft inclination angle, lateral pressure coefficient, and elasticity modulus of lining on the plastic zone radius and radial displacement in the plastic zone are also studied systematically. Research results can provide theoretical guidance to engineering practices.

The remainder of this study is organized as follows. Section 3 elaborates the mechanical analysis modeling process of the cross section of the TBM inclined shaft and derives an elastoplastic solution of lining and surrounding rocks. In Section 4, a parameter analysis is conducted by combining engineering cases, and the influencing laws of intermediate principal stress coefficient, later pressure coefficient of surrounding rocks, and inclined shaft inclination angle on the radius and radial displacement of plastic zone are discussed. Section 5 summarizes the conclusions.

3. Methodology

3.1 Construction of the mechanical analysis model of TBM inclined shaft

The tilt angle of the TBM inclined shaft is recorded as β, as shown in Fig. 1(a). The mechanisms of the lining-surrounding rocks in the cross section 1-1 of the inclined shaft are analyzed. The inclined shaft is relatively long and can be analyzed according to the plane strain problem. The horizontal and vertical stresses in the cross section 1-1 are expressed as σ_y and σ_z in Fig. 1(b). Influenced by β, the initial principal stress direction of rocks is inconsistent with the axial direction of the inclined shaft. To analyze the stresses of surrounding rocks and lining in the cross section 1-1, the coordinate transformation of the initial principal stress of rocks is required (Fig. 2).

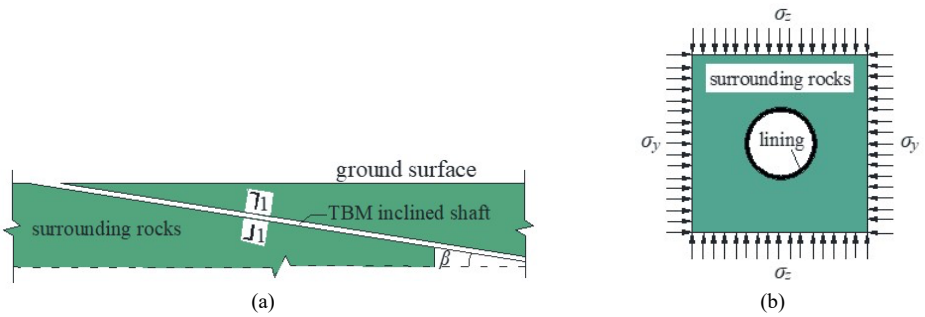

Fig. 1. Location of the inclined shaft and diagram of the cross section. (a) Location of inclined shaft. (b) Cross section 1-1

In Fig. 2, σ_v is the initial vertical principal stress of surrounding rocks. σ_{h1} and σ_{h2} are the horizontal principal stresses. After coordinate transformation, the coordinate system *o–xyz* is acquired. Specifically, the *x*-axis is consistent with the axial direction of the inclined shaft, whereas the *y*- and *z*-axes are consistent with directions of σ_y and σ_z in Fig. 1(b). α is the azimuth angle. The stresses in the *x*, *y*, and *z* directions are σ_x, σ_y, and σ_z, respectively.

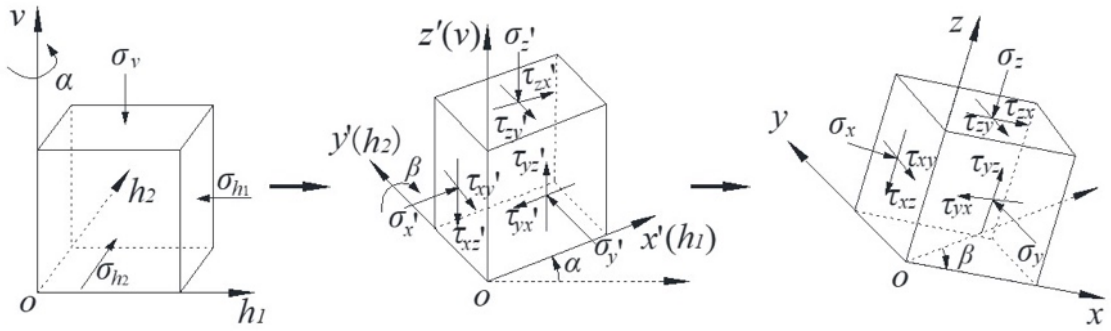

Fig. 2. Coordinate transformation process of the stress of primary rocks

The stress expressions of σ_x, σ_y, and σ_z are shown in Eq. (1).

$$\begin{cases} \sigma_x = \cos^2\beta(\sigma_{h1}\cos^2\alpha + \sigma_{h2}\sin^2\alpha) + \sigma_v\sin^2\beta \\ \sigma_y = \sigma_{h1}\sin^2\alpha + \sigma_{h2}\cos^2\alpha \\ \sigma_z = \sin^2\beta(\sigma_{h1}\cos^2\alpha + \sigma_{h2}\sin^2\alpha) + \sigma_v\cos^2\beta \\ \tau_{xy} = \cos\beta\sin\alpha\cos\alpha(\sigma_{h1} - \sigma_{h2}) \\ \tau_{xz} = \cos\beta\sin\beta(\sigma_{h1}\cos^2\alpha + \sigma_{h2}\sin^2\alpha - \sigma_v) \\ \tau_{yz} = \sin\beta\sin\alpha\cos\alpha(\sigma_{h1} - \sigma_{h2}) \end{cases} \quad (1)$$

The mechanical analysis in this study is based on following hypotheses: (1) Surrounding rocks are isotropic homogeneous continuous media. (2) Surrounding rocks are ideal elastoplastic materials, and the volumetric strain of the plastic zone of surrounding rocks is zero, without considerations to the influence of elastic strain in the plastic zone. (3) Lining is an ideal uniform elastic ring and in tight contact with surrounding rocks, without sliding. (4) The TBM inclined shaft is a deeply buried inclined shaft (buried depth H>20 r_l, where r_l is the inner radius of the inclined shaft).

In this study, the compressive stress is determined positive, and the tensile stress is negative. If the stress difference along the horizontal direction is ignored, then σ_{h1} is equal to σ_{h2} In view of Hypothesis (1), the initial vertical stress (σ_v) is recorded as p_0. Then, horizontal stress σ_{h1} and σ_{h2} are equal to $K_0 p_0$, where K_0 is the lateral pressure coefficient of surrounding rocks. Eq. (1) can be simplified as:

$$\begin{cases} \sigma_x = K_0 p_0\cos^2\beta + p_0\sin^2\beta \\ \sigma_y = K_0 p_0 \\ \sigma_z = K_0 p_0\sin^2\beta + p_0\cos^2\beta \\ \tau_{xy} = 0 \\ \tau_{xz} = (K_0 - 1)p_0\cos\beta\sin\beta \\ \tau_{yz} = 0 \end{cases} \quad (2)$$

The mechanical model of the cross section 1-1 of the inclined shaft is shown in Fig. 3, where r_a is the inner radius of the lining, and r_l is the outer radius of the lining. r_0 is considerably higher than r_l, and p_{lr} is the radial stress between the lining and surrounding rocks.

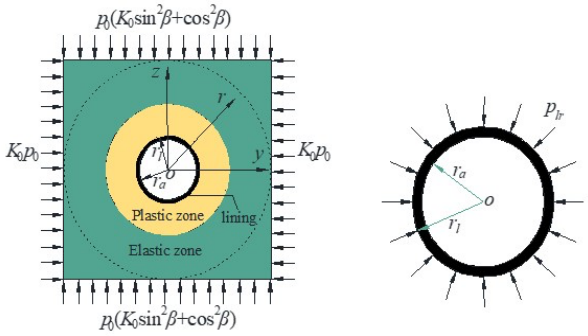

(a) (b)

Fig. 3. Stress models of lining-surrounding rocks. (a) Stress model of cross section 1-1. (b) Stress model of lining

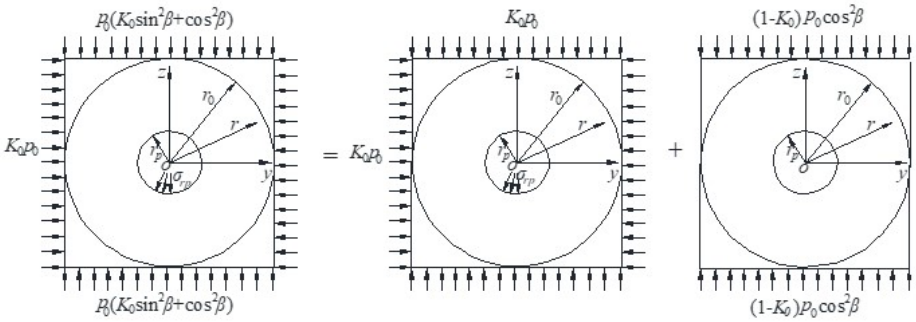

(a) (b) (c)

Fig. 4. Stress analysis model of the elastic zone of surrounding rocks

$$\begin{cases} \sigma_r^e = K_0p_0 - \dfrac{r_p^2}{r_0^2-r_p^2}\left(\dfrac{r_0^2}{r^2}-1\right)(K_0p_0-\sigma_{r_p}) + \dfrac{(1-K_0)p_0\cos^2\beta}{2}\left[\left(1-\dfrac{r_p^2}{r^2}\right)-\left(1-\dfrac{4r_p^2}{r^2}+\dfrac{3r_p^2}{r^4}\right)\cos 2\theta\right] \\ \sigma_\theta^e = K_0p_0 + \dfrac{r_p^2}{r_0^2-r_p^2}\left(\dfrac{r_0^2}{r^2}+1\right)(K_0p_0-\sigma_{r_p}) + \dfrac{(1-K_0)p_0\cos^2\beta}{2}\left[\left(1+\dfrac{r_p^2}{r^2}\right)+\left(1+\dfrac{3r_p^4}{r^4}\right)\cos 2\theta\right] \\ \tau_{r\theta}^e = \dfrac{(1-K_0)p_0\cos^2\beta}{2}\left(1+\dfrac{2r_p^2}{r^2}-\dfrac{3r_p^2}{r^4}\right)\sin 2\theta \end{cases} \tag{3}$$

where σ_r^e is the radial stress of the elastic zone, σ_θ^e is the tangential stress of the elastic zone, $\tau_{r\theta}^e$ is the shearing stress of elastic zone, E is the elasticity modulus of surrounding rocks, μ is the Poisson's ratio of surrounding rocks, σ_{rp} is the radial stress at the border between the elastic and plastic zones, r_0 is the radius of the computational area, and r_p is the plastic zone radius.

Combined with monodromy condition of displacement, the radial displacement u_r^e and tangential displacement u_θ^e of the elastic zone of surrounding rocks can be expressed as follows:

$$\begin{cases} u_r^e = \dfrac{(1+\mu)\left(-\dfrac{r_0^2}{r}-r+2\mu r\right)r_p^2}{E(r_0^2-r_p^2)}\cdot(\sigma_{r_p}-K_0p_0) + \\ \qquad \dfrac{(1+\mu)(1-K_0)p_0\cos^2\beta}{2E}\cdot\left[\dfrac{r_p^2}{r}+\cos 2\theta\left(\dfrac{r_p^4}{r^3}-\dfrac{4(1-\mu)r_p^2}{r}\right)\right] \\ u_\theta^e = \dfrac{(1+\mu)(1-K_0)p_0\cos^2\beta}{2E}\left[\dfrac{r_p^4}{r^3}+\dfrac{2(1-2\mu)r_p^2}{r}\right]\sin 2\theta \end{cases} \tag{4}$$

3.2.2 Solution of stresses and displacement of the plastic zone of surrounding rocks

The unified strength criterion can be expressed as follows [24]:

$$F = \sigma_1\frac{1-\sin\varphi}{1+\sin\varphi} - \frac{1}{1+b}(b\sigma_2+\sigma_3) = \frac{2c\cos\varphi}{1+\sin\varphi} \quad \text{when } \sigma_2 \le \frac{1}{2}(\sigma_1+\sigma_3) - \frac{\sin\varphi}{2}(\sigma_1-\sigma_3) \tag{5}$$

$$F' = \frac{(\sigma_1+b\sigma_2)}{1+b}\frac{1-\sin\varphi}{1+\sin\varphi} - \sigma_3 = \frac{2c\cos\varphi}{1+\sin\varphi} \quad \text{when } \sigma_2 \ge \frac{1}{2}(\sigma_1+\sigma_3) - \frac{\sin\varphi}{2}(\sigma_1-\sigma_3) \tag{6}$$

where c is the cohesive strength of rock, φ is the internal friction angle of rock, b is the influencing coefficient of the intermediate principal stress, σ_1 is the maximum principal stress, σ_2 is the intermediate principal stress, and σ_3 is the minimum principal stress.

There are radial stress (σ_r), tangential stress (σ_θ), and axial stress (σ_z) in surrounding rocks. In the plastic zone, the tangential stress σ_θ^p is the maximum stress, whereas the radial stress σ_r^p is the minimum stress. In other words, σ_1 is equal to σ_θ^p, σ_2 is equal to σ_z^p, and σ_3 is equal to σ_r^p. In plane strain problems, an approximate relationship exists among σ_r^p, σ_θ^p, and σ_z^p, which can be expressed as follows [25]:

$$\sigma_z^p = \frac{\sigma_\theta^p + \sigma_r^p}{2} \tag{7}$$

3.2 Elastoplastic solution of lining-surrounding rocks in the inclined shaft

3.2.1 Solution of stresses and displacements of the elastic zone of surrounding rocks

The stress model of the elastic zone is shown in Fig. 4. The stresses in Fig. 4(a) can be gained by superposing the stress components in Figs. 4(b) and 4(c), as shown in Eq. (3) [23].

From Eqs. (6) and (7), it can be known that

$$\sigma_\theta^p - \sigma_r^p = \frac{4(1+b)\sin\varphi}{(2+b)(1-\sin\varphi)}\sigma_r^p + \frac{4c(1+b)\cos\varphi}{(2+b)(1-\sin\varphi)} \tag{8}$$

In the following text, to simplify the expression, let $A = \frac{4(1+b)\sin\varphi}{(2+b)(1-\sin\varphi)}$ and $B = \frac{4c(1+b)\cos\varphi}{(2+b)(1-\sin\varphi)}$.

The stresses in the plastic zone of surrounding rocks have weak relationship with the initial stresses of surrounding rocks. It is mainly determined by the ultimate balance condition of rock failure, and it is related with the tunnel shape. Hence, the plastic zone is calculated according to the axial symmetric state of the plane. Stresses in the plastic zone meet the balance differential equation:

$$\frac{d\sigma_r^p}{dr} + \frac{\sigma_r^p - \sigma_\theta^p}{r} = 0 \tag{9}$$

The boundary condition of stresses at the contact surface between the elastic and plastic zones is shown as follows:

$$\sigma_{r|r=r_p}^p = \sigma_{r|r=r_p}^e = \sigma_{rp} \tag{10}$$

Combining Eqs. (8)–(10), the expression of radial stress σ_r^p and tangential stress σ_θ^p in the plastic zone can be deduced as follows:

$$\begin{cases} \sigma_r^p = (\frac{r}{r_p})^A(\sigma_{rp} + c\cdot\cot\varphi) - c\cdot\cot\varphi \\ \sigma_\theta^p = (1+A)(\frac{r}{r_p})^A(\sigma_{rp} + c\cdot\cot\varphi) - c\cdot\cot\varphi \end{cases} \tag{11}$$

The stresses of the elastic zone at the border between the elastic and plastic zones meet the yield strength criterion. Combining Eqs. (3) and (8), σ_{rp} becomes

$$\sigma_{r_p} = \frac{\frac{2r_0^2}{r_0^2 - r_p^2}K_0 p_0 + (1-K_0)p_0\cos^2\beta(1+2\cos2\theta) - B}{A + \frac{2r_0^2}{r_0^2 - r_p^2}} \tag{12}$$

The non-associated flow rule is applied to solve the displacement of the plastic zone. In view of Hypothesis (2), the non-associated flow rule can be simplified as

$$\varepsilon_r^p + \varepsilon_\theta^p = 0 \tag{13}$$

where ε_r^p is the radial strain in the plastic zone, and ε_θ^p is the tangential strain in the plastic zone. The elastic displacement ($u_{r|r=r_p}^e$) and plastic displacement ($u_{r|r=r_p}^p$) of surrounding rocks at the border between the elastic and plastic zones meet the displacement continuity condition $u_{r|r=r_p}^p = u_{r|r=r_p}^e$.

Finally, the radial displacement of plastic zone u_r^p can be expressed as follows:

$$\begin{aligned} u_r^p = {} & \frac{(1-\mu-2\mu^2)K_0 p_0}{E}[\frac{r_p^2}{r} - r] + \frac{r_p^2}{r}\frac{(1+\mu)(-r_0^2 - r_p^2 + 2\mu r_p^2)}{E(r_0^2 - r_p^2)}(\sigma_{r_p} - K_0 p_0) + \\ & \frac{(1+\mu)(1-K_0)p_0\cos^2\beta}{E}\cdot[\frac{r_p^2}{r}(1-\mu)(1-2\cos2\theta) - r(\sin^2\theta - \mu)] \end{aligned} \tag{14}$$

3.2.3 Solution of stresses and displacement of lining

In view of the above hypotheses and analysis, the lining structure only has elastic deformation, and it is in the axial symmetric stress state. It is calculated according to the thick-wall cylinder structure. Stresses and displacement in lining are expressed as follows:

$$\begin{cases} \sigma_r^l = \frac{r_l^2(r^2 - r_a^2)}{r^2(r_l^2 - r_a^2)}p_{lr} \\ \sigma_\theta^l = \frac{r_l^2(r^2 + r_a^2)}{r^2(r_l^2 - r_a^2)}p_{lr} \end{cases} \tag{15}$$

$$u_r^l = \frac{(1+\mu)p_{lr}}{E_l}\frac{r_l^2(r^2 + r_a^2 - 2\mu r^2)}{r(r_l^2 - r_a^2)} \tag{16}$$

where σ_r^l is the radial stress of lining, σ_θ^l is the tangential stress of the lining, u_r^l is the radial displacement of the lining, p_{lr} is the support force of lining, and E_l is the elasticity modulus of lining.

The stresses and displacements continuity boundary conditions between the lining and surrounding rocks can be expressed as

$$\begin{cases} \sigma_{r|r=r_l}^p = \sigma_{r|r=r_l}^l = p_{lr} \\ u_{r|r=r_l}^p = u_{r|r=r_l}^l = u_{lr} \end{cases} \tag{17}$$

Therefore, r_p and p_{lr} can be calculated by combining Eqs. (11), (12), and (14)–(17). r_p and p_{lr} are brought into Eqs. (3) and (4) to obtain σ_r^e, σ_θ^e, $\tau_{r\theta}^e$, u_r^e, and u_θ^e, which can be brought into Eqs. (11) and (14) to calculate σ_r^p, σ_θ^p, and u_r^p. The above equations are mainly transcendental and are calculated using Matlab software.

4. Result Analysis and Discussion

A TBM inclined shaft project in China was selected to analyze the mechanical characteristics of surrounding rocks. The values of the parameters are listed in Table 1.

Table. 1. Parameter values of the TBM inclined shaft

r_a (m)	r_l (m)	r_0 (m)	c (MPa)	φ (°)	μ	p_0 (MPa)	E (GPa)
3.3	3.65	60	2.2	22	0.2	7	1

4.1 Effect of b on r_p and u_r^p

When K_0=1, the plastic zone is round. The influencing curves of b on r_p and u_r^p are shown in Fig. 5. The results show that r_p decreases obviously with the increase of b. When b increases from 0 to 1, r_p/r_l decreases by 9.96%, from 1.205 to 1.085. The maximum value of u_r^p is achieved at the shaft wall, and it decreases gradually with the increase of the radius. At the same position, u_r^p decreases with the increase of b. When b increases from 0 to 1, the radial displacement of the shaft wall decreases by 18%. Hence, considering intermediate principal stress, the stability of surrounding rocks is strengthened. When b=0, the unified strength criterion is degraded into the M–C strength criterion. Thus, the results calculated based on the M–C strength criterion are relatively conservative. Although such conservative results are beneficial for engineering safety, they increase the requirements on support strength to some extent, as well as the construction cost.

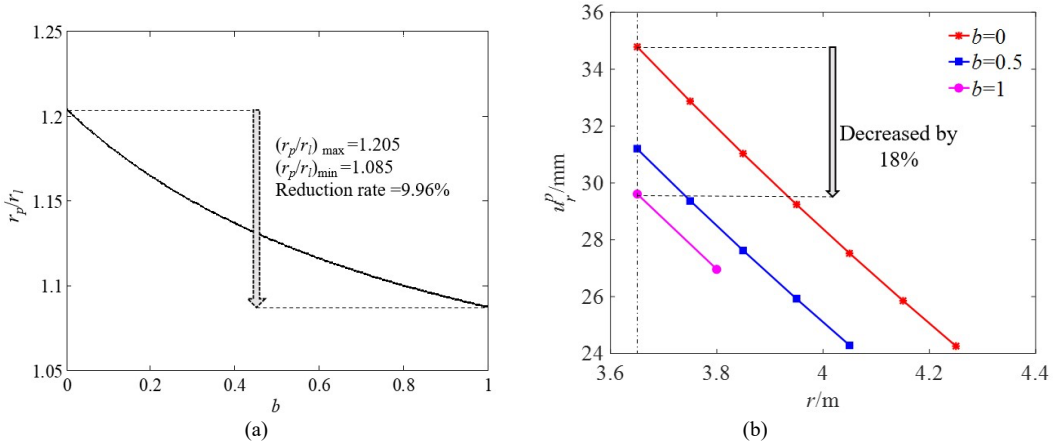

Fig. 5. Effect of b on r_p and u_r^p. (a) Effect of b on r_p. (b) Effect of b on u_r^p

4.2 Effect of K_0 on r_p and u_r^p

When $K_0 \neq 1$, the plastic zone of surrounding rocks is symmetric around the rectangular coordinates. Hence, only the plastic zone in the first quadrant was analyzed in this study. As shown in Fig. 6(a), when K_0=0.7, r_p in the horizontal direction is the maximum, and it decreases gradually along the counterclockwise direction until it disappears at an angle. In view of the curves in Fig. 6(b), r_p in the vertical direction is the maximum when K_0=1.3, and it decreases gradually along the clockwise direction. The plastic zone disappears until it reaches the horizontal direction. The results also show that the plastic zone of surrounding rocks is smaller when the intermediate principal stress is greater.

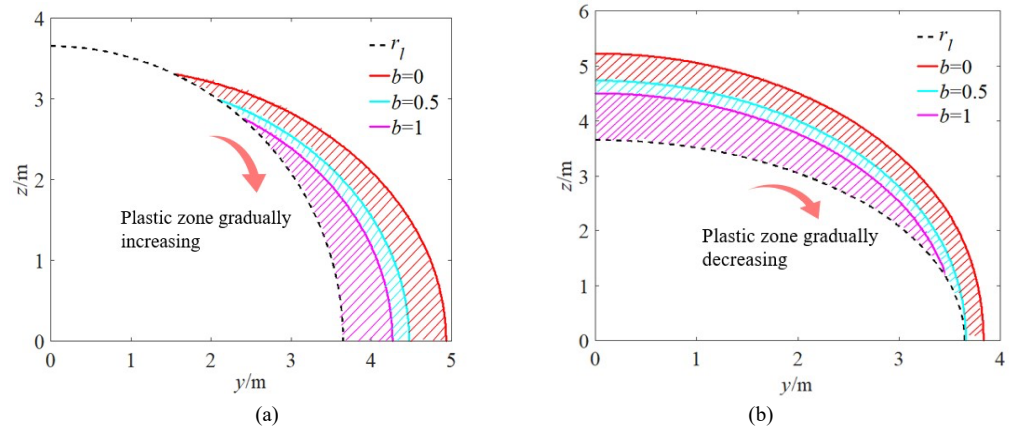

Fig. 6. Effects of K_0 and b on r_p. (a) K_0=0.7. (b) K_0=1.3

Variations of u_r^p with K_0 and b are shown in Fig. 7. With the increase of K_0, u_r^p in the horizontal direction increases significantly, whereas u_r^p in the vertical direction decreases gradually. When b=0, u_r^p in the horizontal direction increases by 83%, and u_r^p in the vertical direction decreases by 14% when K_0 increases from 0.8 to 1.2. When b=1, u_r^p in the horizontal direction increases by 40%, and u_r^p in the vertical direction decreases significantly when K_0 increases from 0.8 to 1.2. When K_0=0.8, the plastic zone in the vertical direction of surrounding rocks disappears. To sum up, r_p and u_r^p change greatly with K_0, which can influence the engineering safety of deeply buried inclined shaft significantly. It shall determine the reasonable value of K_0 in engineering by combining with practical situations.

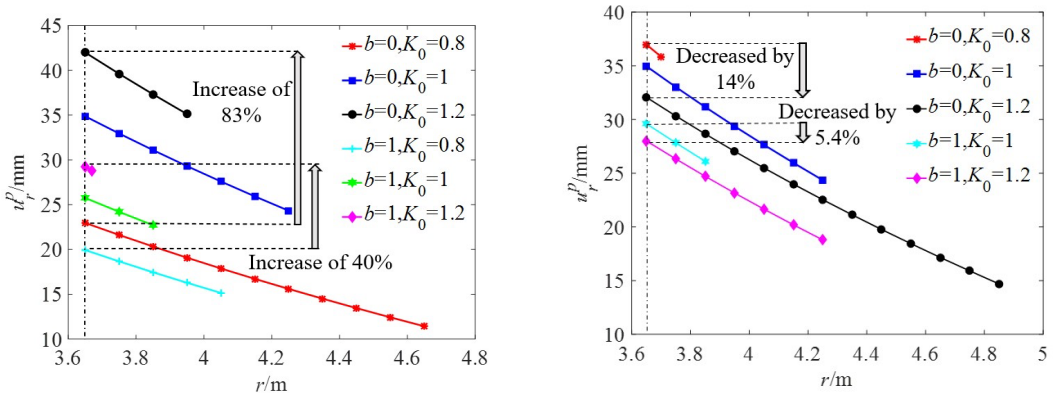

Fig. 7. Effects of K_0 and b on u_r^p. (a) u_r^p in horizontal direction. (b) u_r^p in vertical direction

4.3 Effect of β on r_p and u_r^p

In this study, β was set to 0°, 8°, 16° and 24°. Variations of r_p with β when b=0.5 and K_0 is 0.7 and 1.3 are shown in Fig. 8. The results are analyzed as follows. When K_0=0.7, r_p in the horizontal direction decreases with the increase of β, but the variation amplitude is relatively small. No plastic zone is present along the vertical direction. When K_0=1.3, r_p in the horizontal direction increases with β, whereas r_p in the vertical direction decreases, but the variation amplitudes are small. When b=0 and K_0=1.3, plastic zones are present on the horizontal and vertical directions of surrounding rocks. Hence, the influencing laws of β on the u_r^p in the horizontal and vertical directions were investigated by fixing b=0 and K_0=1.3. The results are shown in Fig. 9. u_r^p in the horizontal and vertical directions increases with β, but the u_r^p in the vertical direction changes greatly. Moreover, the u_r^p increases more significantly when β is greater. The results have important influences to engineering safety and lining structural design.

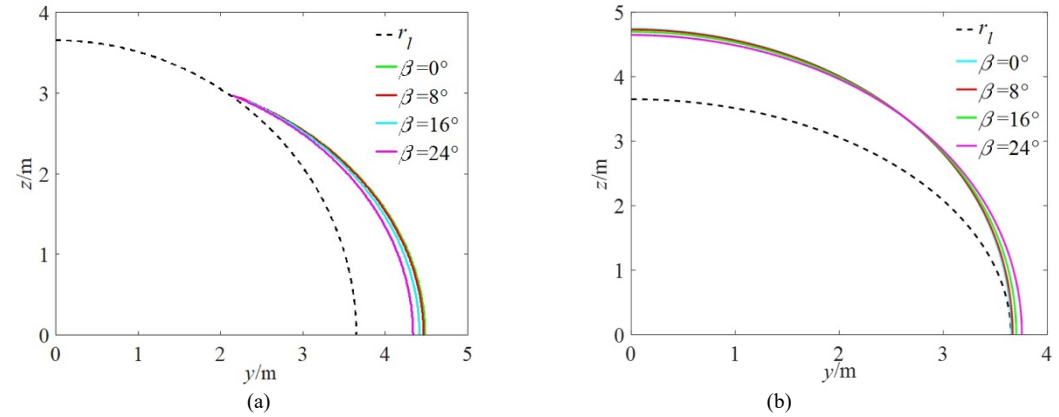

Fig. 8. Effect of β on r_p. (a) K_0=0.7. (b) K_0=1.3

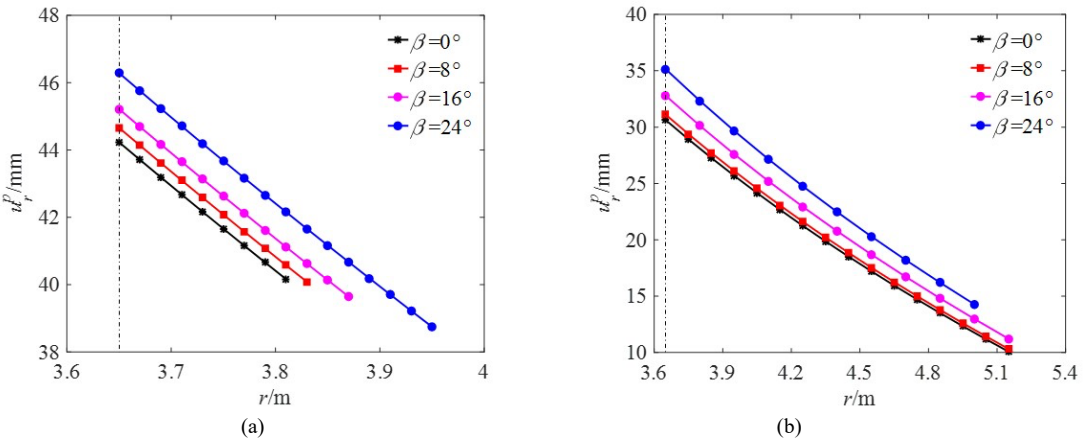

Fig. 9. Effect of β on u_r^p. (a) u_r^p in horizontal direction. (b) u_r^p in vertical direction

4.4 Effect of E_l / E on r_p and u_r^p

Different support structures have varied resistance to deformation and provide different supporting effects to surrounding rocks. Investigating the influencing laws of E_l / E on r_p and u_r^p have important significance to the support design and stability evaluation of surrounding rocks.

The variation laws of r_p with E_l / E when b is equal to 0, 0.5, and 1 are shown in Fig. 10(a). With the increase of E_l / E, r_p decreases obviously. When E_l / E increases to 3, the plastic zone disappears. As shown in Fig. 10(b), u_r^p decreases sharply with the increase of E_l / E. When b=0 and E_l / E increases from 0.5 to 3, the radial displacement at the tunnel wall can be decreased by 44%. When b=1 and E_l / E increases from 0.5 to 2, the radial displacement of the tunnel wall can be decreased by 26%. Therefore, r_p and u_r^p may decrease with the increase of E_l / E, whereas the supporting force increases significantly.

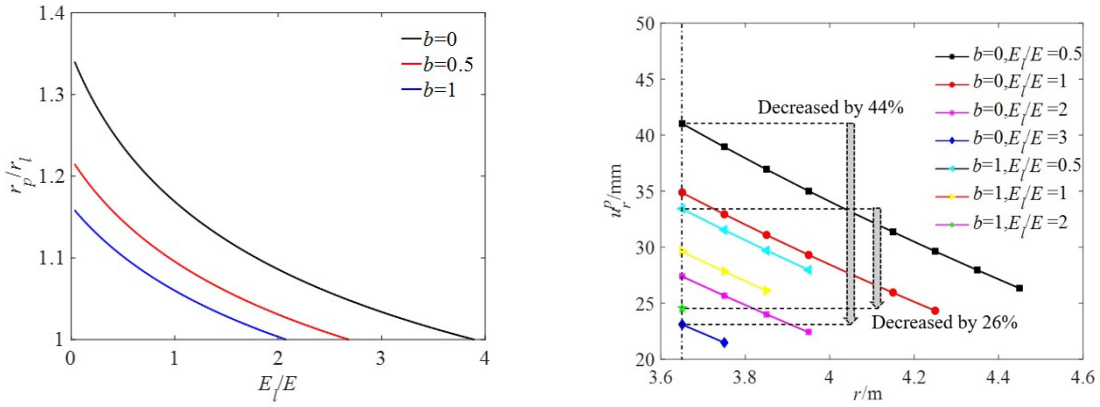

Fig. 10. Effect of E_l / E on r_p and u_r^p. (a) Effect of E_l / E on r_p. (b) Effect of E_l / E on u_r^p

5. Conclusions

To explore the mechanical properties of surrounding rocks and lining structure after excavation of the TBM inclined shaft, a mechanical analysis model of the cross section of the shaft was constructed, and a parameter analysis was performed using an engineering case. The influencing laws of b, K_0, β and E_l / E on r_p and u_r^p were discussed. Some major conclusions could be drawn as follows.

(1) The elastoplastic solution of lining-surrounding rocks in the TBM inclined shaft was deduced based on unified strength theory. It comprehensively reflects the influences of intermediate principal stress, lateral pressure coefficient of surrounding rocks, angle of the inclined shaft, and elasticity modulus of lining on r_p and u_r^p.

(2) The lateral pressure coefficient of surrounding rocks and the elasticity modulus of lining significantly affect r_p and u_r^p. The angle of the inclined shaft mainly influences the u_r^p in vertical direction. The parameter values in engineering can be determined according to practical conditions.

(3) When the effect of intermediate principal stress is considered, r_p and u_r^p decrease obviously with the increase of the intermediate principal stress, and the stability of the surrounding rocks in the TBM inclined shaft is strengthened obviously.

On the basis of the comprehensive analysis of several factors, the theoretical solution is closer to practical situations. It has relatively extensive theoretical significance and can provide some references to similar engineering. This study makes a mechanical analysis based on the hypothesis that the lining structure is a uniform elastic ring. However, it lacks deep discussion on the characteristics of lining structure. Further studies on the number of joints and positions of lining are needed. Moreover, the support structure shall be optimized by combining with numerical calculations.

Acknowledgements

The authors are grateful for the support provided by the Scientific Research Fund of Qingdao Agricultural University (Grant No. 663/1120055).

References

[1] T. L. Cheng and M. Yao, "Application and development of TBM in coal nine construction," *Eng. Technol. Res.*, vol. 7, no. 13, pp. 115-117, Jul. 2022.

[2] E. Komurlu, A. Kesimal, and R. Hasanpour, "In situ horizontal stress effect on plastic zone around circular underground openings excavated in elastic zones," *Geomech. Eng.*, vol. 8, no. 6, pp. 783-799, Jun. 2015.

[3] H. N. Wang, Y. Li, L. S. Luo, M. J. Jiang, and G. S. Zeng, "Analytical research of mechanical response of TBM construction in strain-softening elasto-plastic rock," *Chin. J. Rock. Mech. Eng.*, vol. 35, no. 2, pp. 356-368, Feb. 2016.

[4] S. K. Sharan, "Analytical solutions for stresses and displacements around a circular opening in a generalized Hoek-Brown rock," *Int. J. Rock. Mech. Min.*, vol. 45, no. 1, pp. 78-85, Jan. 2008.

[5] R. Chen and F. Tonon, "Closed-form solutions for a circular tunnel in elastic–brittle–plastic ground with the original and generalized Hoek–Brown failure criteria," *Rock. Mech. Rock. Eng.*, vol. 44, no. 2, pp. 169-178, Mar. 2011.

[6] X. B. Zhang, G. M. Zhao, and X. R. Meng, "Elastoplastic analysis of surrounding rock on circular roadway based on Drucker-Prager yield criterion," *J. Chin. Coal. Soc.*, vol. 38, no. s1, pp. 30-37, Apr. 2013.

[7] X. F. Guo, Z. Q. Zhao, X. Gao, X. Y. Wu, and N. J. Ma, "Analytical solutions for characteristic radii of circular roadway surrounding rock plastic zone and their application," *Int. J. Min. Sci. Techno.*, vol. 29, no. 2, pp. 263-272, May. 2019.

[8] B. Haimson and C. Chang, "A new true triaxial cell for testing mechanical properties of rock, and its use to determine rock strength and deformability of Westerly granite," *Int. J. Rock. Mech. Min.*, vol. 37, no. 1-2, pp. 285-296, Jan. 2000.

[9] Z. S. Zou, J. Yang, Z. M. Wang, and H. Y. Liu, "The plastic zone of tunnel surrounding rock under unequal stress in two directions based on the unified strength theory," *Math. Probl. Eng.*, vol. 2021, pp. 1-11, Feb. 2021, Art. no. 8842153.

[10] K. Park, "Simple solutions of an opening in elastic–brittle plastic rock mass by total strain and incremental approaches," *Geomech. Eng.*, vol. 13, no. 4, pp. 585-600, Oct. 2017.

[11] A. Singh, K. S. Rao, and R. Ayothiraman, "An analytical solution to wellbore stability using Mogi–Coulomb failure criterion," *J. Rock. Mech. Geotech.*, vol, 11, no. 6, pp. 1211-1230, Dec. 2019.

[12] A. Hedayat and J. Weems, "The elasto-plastic response of deep tunnels with damaged zone and gravity effects," *Rock. Mech. Rock. Eng.*, vol. 52, no. 12, pp. 5123-5135, Dec. 2019.

[13] A. Adhikari and N. Roy, "Influence of anisotropic stress conditions on tunnel deformation and sequential excavation performance in rock mass," *J. Geol. Soc. India.*, vol. 99, no.7, pp. 965-974, Jul. 2023.

[14] Y. C. Ma, A. Z. Lu, and H. Cai, "An analytical method for determining the non-enclosed elastoplastic interface of a circular hole," *Math. Mech. Solids.*, vol. 25, no. 5, pp. 1199-1213, May. 2020.

[15] H. H. Chen, H. H. Zhu, and L. Y. Zhang, "Analytical Solution for deep circular tunnels in rock with consideration of disturbed zone, 3D strength and large strain," *Rock. Mech. Rock. Eng.*, vol. 54, no. 3, pp. 1391-1410, Mar. 2021

[16] N. J. Ma, J. Li, and Z. Q. Zhao, "Distribution of the deviatoric stress field and plastic zone in circular roadway surrounding rock," *Chin. J. Univ. Min. Techno.*, vol. 44, no. 2, pp. 206-213, Mar. 2015.

[17] B. Behnam, S. Fazlollah, and M. Hamid, "Prediction of plastic zone size around circular tunnels in non-hydrostatic stress field," *Int. J. Min. Sci. Techno.*, vol. 24, no. 1, pp. 81-85, Jan. 2014.

[18] Y. K. Lee and S. Pietruszczak, "A new numerical procedure for elasto-plastic analysis of a circular opening excavated in a strain-softening rock mass," *Tunn. Undergr. Sp. Tech.*, vol. 23, no. 5, pp. 588-599, May. 2008.

[19] K. H. Zeng, X. J. Li, S. S. Lu, and H. L. Li, "Unified plastic solutions to a circular tunnel under two-way unequal pressures and their applications," *Chin. J. Geotech. Eng.*, vol. 44, no. 10, pp. 1772-1779, Oct. 2022.

[20] Y. Yuan, Z. H. Liu, C. Zhu, C. F. Yuan, and S. Z. Wang, "The effect of burnt rock on inclined shaft in shallow coal seam and its control technology," *Energy. Sci. Eng.*, vol. 7, no. 5, pp. 1882-1895, Jul. 2019.

[21] S. X. Qiao, Z. W. Peng, J. K. Zhang, and L. H. Jin, "Parameter calibration and system design of material lifting system for inclined shaft construction," *Appl. Sci-Basel.*, vol. 13, no. 17, Sep. 2023, Art. no. 9909.

[22] J. D. Fan *et al*., "Key technology and equipment of intelligent mine construction of whole mine mechanical rock breaking in Kekegai Coal Mine," *J. Chin. Coal. Soc.*, vol. 47, no. 1, pp. 499-514, Jan. 2022.

[23] Y. Pan, G. M. Zhao, and X. R. Meng, "Elasto-plastic analysis on surrounding rock mass under non-uniform stress field," *J. Chin. Coal. Soc.*, vol. 36, no. s1, pp. 53-57, May. 2011.

[24] X. H. Cai, H. P. Kang, Y. P. Cai, and Y. B. Cai, "Elastoplastic calculation of adjoining rock and lining for undersea tunnel considering effect of intermediate principal stress," *Chin. J. Rock. Soil. Mech.*, vol. 31, no. 10, pp. 3209-3216, Oct. 2010.

[25] S. Q. Xu and M. H. Yu, "The Effect of the intermediate principal stress on the ground response of circular openings in rock mass," *Rock. Mech. Rock. Eng*., vol. 39, no. 2, pp. 169-181, Apr. 2006.